J MATER RES TECHNOL. 2016;5(4):353–359

Available online at www.sciencedirect.com

jmr&t Journal of Materials Research and Technology

www.jmrt.com.br

Original Article

A comparison of repetitive corrugation and straightening and high-pressure torsion using an Al-Mg-Sc alloy

Prabhakar M. Bhovi[a], *Deepak C. Patil*[b], *S.A. Kori*[c], *K. Venkateswarlu*[d], *Yi Huang*[e,*], *Terence G. Langdon*[e]

[a] *B.V. Bhoomaraddi College of Engineering and Technology, Hubballi, India*
[b] *KLE Dr. M.S. Sheshgiri College of Engineering and Technology, Belagavi, India*
[c] *Basaveshwar Engineering College, Bagalkot, India*
[d] *CSIR-National Aerospace Laboratories, Bangalore, India*
[e] *Materials Research Group, Faculty of Engineering and the Environment, University of Southampton, Southampton, United Kingdom*

ARTICLE INFO

Article history:
Received 7 January 2016
Accepted 30 March 2016
Available online 14 June 2016

Keywords:
Al-Mg-Sc alloy
High-pressure torsion
Homogeneity
Repetitive corrugation and straightening
Ultrafine grains

ABSTRACT

A comparative study was conducted to evaluate the influence of two different severe plastic deformation (SPD) processes: repetitive corrugation and straightening (RCS) and high-pressure torsion (HPT). Samples of an Al-3Mg-0.25Sc alloy with an initial grain size of ~150 μm were processed by RCS through 8 passes at room temperature either without any rotation during processing or with a rotation of 90° around the longitudinal axis between each pass. Thin discs of the alloy were also processed for up to 5 turns by HPT at room temperature. The results show that both procedures introduce significant grain refinement with average grain sizes of ~0.6–0.7 μm after RCS and ~95 nm after HPT. Measurements of the Vickers microhardness gave values of ~128 after RCS and ~156 after HPT. The results demonstrate that processing by HPT is the optimum processing technique in achieving both high strength and microstructural homogeneity.

1. Introduction

Various severe plastic deformation (SPD) techniques are now available for achieving ultrafine-grained (UFG) metals with grain sizes in the submicrometer or nanometer ranges [1]: examples of these techniques include equal-channel angular pressing (ECAP) [2], high-pressure torsion (HPT) [3], accumulative roll bonding (ARB) [4], multi-directional forging [5] and multi-axial compression (MAC) [6]. A significant advantage of SPD processing is that it involves procedures in which bulk metals are subjected to very high strains but without introducing any significant change in their overall geometries. Thus, these procedures are now attracting considerable attention because of their potential for introducing exceptional mechanical and functional properties [7–11].

* *Corresponding author.*
E-mail: y.huang@soton.ac.uk (Y. Huang).
http://dx.doi.org/10.1016/j.jmrt.2016.03.009

Recently, much attention has focused on processing by HPT because this procedure produces grains that are exceptionally small [12,13] and the grains generally have high fractions of high-angle grain boundaries [14]. Nevertheless, a disadvantage with HPT is that the samples are usually in the form of very thin discs and there are difficulties associated with scaling the processing to involve larger cylindrical samples [15,16].

An alternative and relatively simple SPD procedure is repetitive corrugation and straightening (RCS), which was first introduced more than ten years ago [17,18]. In this process, a sample in the form of a sheet is repetitively bent and straightened without significantly changing the cross-sectional geometry and thereby the process introduces a large plastic strain which leads to grain refinement. It is well established that the RCS process produces bulk nanostructured materials that are free of any contaminants or porosity. Furthermore, processing by RCS appears to be appropriate for use in large-scale industrial applications as, for example, in the production of fuselage structures in the aerospace industry. Nevertheless, to date there are only a limited number of reports describing investigations using RCS processing. Early investigations of RCS evaluated the process with pure Cu [17–19] but later experiments used pure Al and Al-0.25% Sc [20], Cu-2% Ni-1% Si [21–23], a Co superalloy [24], Cu-0.6% Cr [22,25–27], Cu-30% Zn [27], Cu-37% Zn [23], Al-4% Cu-2% Sc [28] and an AA2024 Al-Cu alloy [28].

Although processing by HPT is generally regarded as the optimum SPD process for producing exceptional grain refinement, there has been no attempt so far to make a critical comparison of the microstructures that are produced using HPT and RCS. Accordingly, the present research was initiated to provide a detailed comparison between these two SPD techniques with special emphasis on the grain sizes and the levels of homogeneity that may be achieved. In addition, hardness values were compared by taking measurements of the Vickers microhardness both across diameters of HPT discs and along the lengths of RCS samples. The experiments were conducted using an Al-3% Mg-0.25% Sc alloy, where this material was selected because there are numerous experiments showing Al-Mg-Sc alloys are easily processed by HPT [29–31] and earlier experiments demonstrated the successful processing of aluminium-based alloys by RCS [20,28].

2. Experimental material and procedures

Selected quantities of commercial purity (99.99%) aluminium, an Al-2 wt.% Sc alloy and an Al-3 wt.% Mg alloy were melted in a graphite crucible in an electrical resistance furnace at 1073 K. The melt was then maintained at 973 K for 10 min before pouring into a metal mould to obtain an as-cast Al-3Mg-0.25Sc alloy, which was homogenized at 758 K for 24 h. In this condition, the average initial grain size determined by optical microscopy was ~150 μm, which is consistent with earlier reports for cast Al-Mg-Sc alloys [32,33]. Samples were cut into blocks with dimensions of $80 \times 12 \times 12\ mm^3$ for RCS processing and rods were prepared with diameters of 10.5 mm and lengths of 90 mm for subsequent HPT processing.

For RCS, the block samples were subjected to a repetitive bending and straightening operation in which the straightening restored the initial shape. Each sample was processed through a total of eight passes at room temperature (298 K) either without any rotation during processing or with a rotation of 90° in the same sense around the longitudinal axis between each separate pass. For processing by HPT, the rods were machined to diameters of 10 mm and then sliced into discs with thicknesses of ~1 mm. These discs were polished to final thickness of ~0.85 mm and then processed using an HPT facility operating under quasi-constrained conditions [34,35] in which the disc is held under an applied pressure between two massive anvils and there is a limited outward flow of material around the periphery of the disc during processing. The HPT was conducted at room temperature under an applied pressure of 6.0 GPa with a rotational speed of 1 rpm and for different numbers of turns, N, up to a maximum of 5 turns.

The samples processed by RCS and HPT were evaluated in different ways as illustrated in Fig. 1 where the RCS sample is shown at the top and the HPT sample at the bottom. For the as-cast and RCS processed samples, the Vickers microhardness, Hv, was recorded along linear traverses on each sample using a METATEK hardness tester. These measurements were recorded along a central longitudinal line at incremental separations of 10 mm using a load of 0.5 kgf and a dwell time for each measurement of 10 s. For the HPT discs, the samples were prepared to a mirror-like condition and then Vickers hardness measurements were recorded along diameters of the samples at incremental separations of 0.5 mm using a Micro-DUROMAT400039 facility with a load of 100 g and a dwell time of 15 s. Following conventional practice [36], individual hardness values were recorded at four selected points approximately equally spaced around each point of measurement. Thus, it is apparent from Fig. 1 that the incremental spacing between the microhardness indentations were 10 and 0.5 mm for the RCS and HPT samples, respectively.

Small discs of ~3 mm diameter were prepared for transmission electron microscopy (TEM) at the positions indicated on the RCS and HPT samples in Fig. 1 where these observations were conducted near the ends of the blocks for the RCS samples and at the centres and edge positions for the HPT samples. All discs were mechanically ground and then electropolished using a perchloric acid–ethanol mixture. The TEM observations were conducted using a JEOL JEM 2100 instrument operating at a voltage of 200 kV.

3. Experimental results

In order to evaluate the significance of microstructural inhomogeneities in samples processed by these two different SPD techniques, it is now well established that the most convenient approach is to take measurements of the local microhardness at selected points and to undertake a series of microstructural observations using TEM [37–40]. Adopting this approach, the following section describes the results obtained using RCS processing and the next section describes the results from HPT processing.

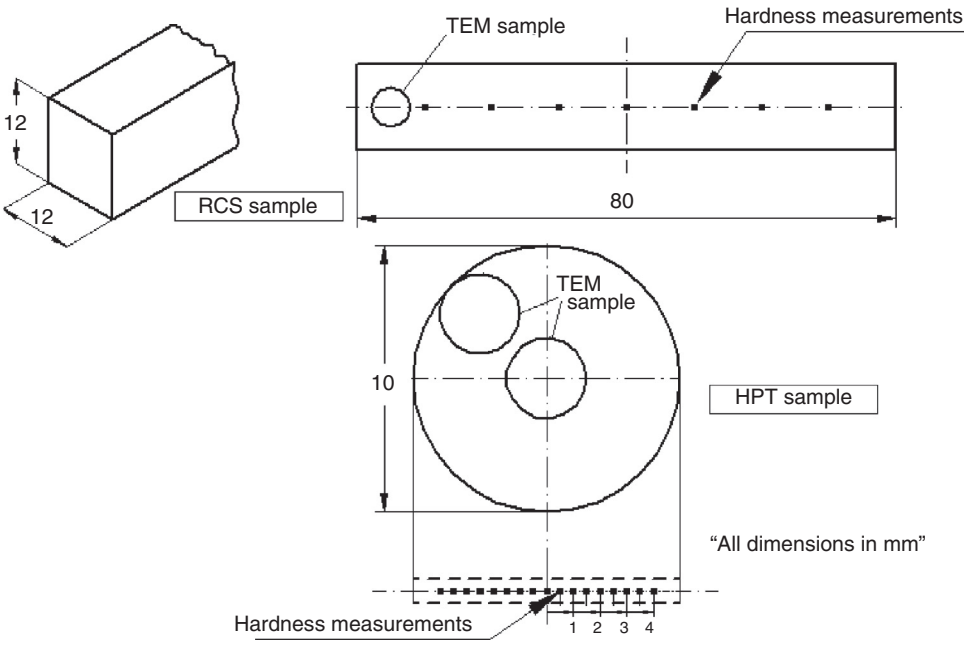

Fig. 1 – Schematic illustrations of the hardness measurement points and the positions for the TEM samples for the RCS (upper) and HPT (lower) samples.

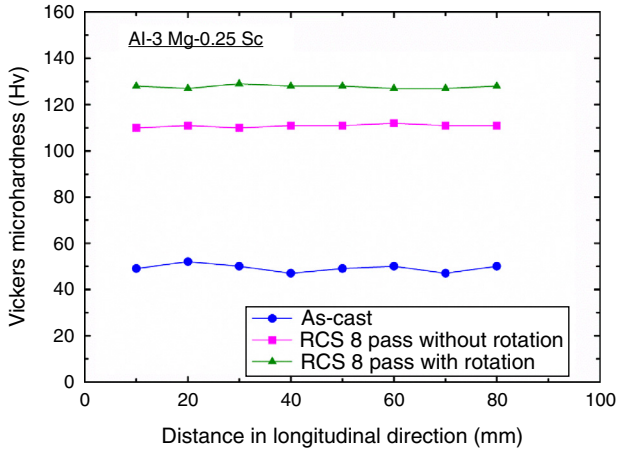

Fig. 2 – Values of the Vickers microhardness for the as-cast alloy and the alloy processed by 8 passes of RCS with and without rotation plotted against the distance measured on the samples in a longitudinal direction.

3.1. *Hardness and microstructural evolution in RCS processing*

The average microhardness values recorded along the central longitudinal sections of the RCS samples are shown in Fig. 2 where the lower line denotes the initial as-cast condition and the two upper lines show measurements taken on the RCS samples after 8 passes either with or without rotation during processing. These results show that the initial hardness is Hv ≈ 50 but the hardness is increased to a much higher value of Hv ≈ 110 after RCS through 8 passes without rotation and then further increased to Hv ≈ 128 if the block is rotated by 90° between passes. This beneficial effect of sample rotation during SPD processing is not generally recognized in RCS but it is consistent with earlier results demonstrating the advantage of sample rotation when processing using ECAP [41,42]. An important conclusion from Fig. 2 is that RCS leads both to high hardness and, more importantly, to hardness values that are essentially uniform throughout the length of the sample. Since the sample is bent and straightened in each pass, there is no appreciable change in the overall dimensions and it is anticipated that a large plastic strain is introduced, which leads ultimately to a constant level of deformation throughout the sample. In addition, it is anticipated that the hardness remains fairly uniform along the thickness in the transverse plane of specimens processed by RCS [43].

A representative TEM micrograph is shown in Fig. 3 for the RCS sample processed through 8 passes without rotation together with the corresponding selected area electron diffraction (SAED) pattern. Detailed measurements showed that processing by RCS produced very substantial grain refinement with an average grain size of ~0.7 μm when processed without rotation. Measurements suggested a slightly smaller grain size of ~0.6 μm when using rotation between each pass. As noted in Fig. 3, there was a tendency for the presence of some elongated grains and a high dislocation density when processing without rotation. In general, all observations showed that the grain boundaries after RCS were wavy and diffuse and this matches earlier reports for materials processed by ECAP [44,45]. It is well established that this corresponds to the introduction of non-equilibrium boundaries having high energies and an excess of extrinsic dislocations [46,47].

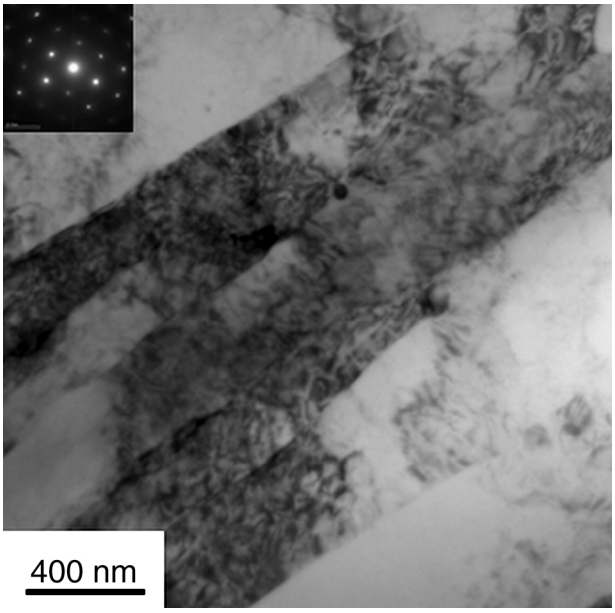

Fig. 3 – TEM image showing representative microstructure and SAED pattern after processing by RCS for 8 passes without rotation.

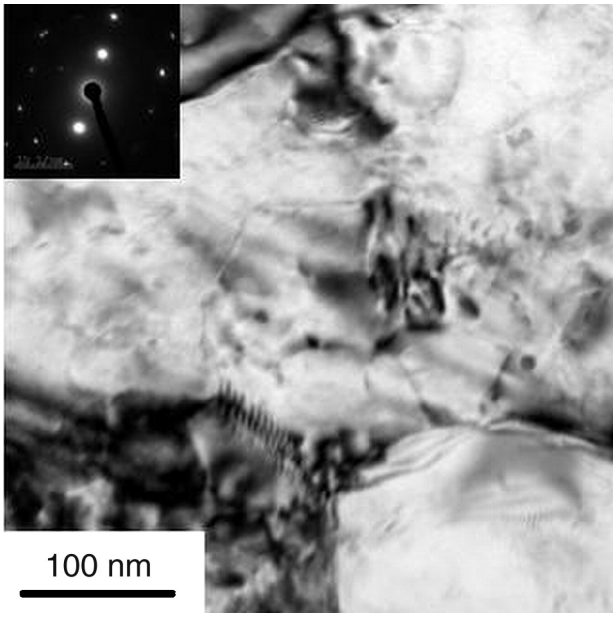

Fig. 5 – TEM image showing representative microstructure and SAED pattern after processing by HPT for 1 turn in the edge region of the disc.

3.2. *Hardness and microstructural evolution in HPT processing*

Processing by HPT produces a very significant strengthening as shown by the microhardness measurements recorded in Fig. 4: again, the lower line denotes the as-cast material at Hv ≈ 50 and the upper lines depict the recorded hardness values obtained at incremental spacing of 0.5 mm for samples processed through 1/2 to 5 turns.

Two significant conclusions may be reached from inspection of the data in Fig. 4. First, the hardness values are initially low near the centre of the disc and high at the edge but gradually the values increase near the centre until ultimately, after 5 turns, the hardness values are fairly uniform across the disc diameter with Hv ≈ 150–156. During this straining, the hardness remains reasonably constant at the edge of the disc but increases substantially in the central region. This evolution towards a uniform distribution of hardness values is consistent with theoretical predictions for HPT processing based on strain gradient plasticity modelling [48]. The tendency for lower hardness values to occur initially in the centres of the discs is consistent with many earlier reports for several different materials including Al [49] and Cu [50,51] alloys and the gradual evolution towards saturation hardness is also well documented in many metals [52–54]. Thus, the present results show that a reasonable level of homogeneity is achieved after 5 turns of HPT. Second, the final hardness after 5 turns is Hv ≥ 150 and, by considering Fig. 2, this value is significantly higher than the maximum hardness achieved in RCS processing after 8 passes with rotation of the sample after every pass. Therefore, these results confirm the advantage of processing by HPT by comparison with RCS. A representative TEM micrograph and SAED pattern is shown in Fig. 5 recorded at the edge of the disc after processing through only 1 turn. For this condition, several observations showed arrays of ultrafine grains with a measured average size of ~95 nm. From the corresponding SAED patterns there was evidence for the presence of many small grains having multiple orientations within each field of view. It is readily apparent by inspection of Fig. 4 that the condition in Fig. 5 is very close to the saturation condition for this alloy since the edge region saturates in the very early stages of HPT processing. In general, the microstructure in the central region appeared to be coarser with an ill-defined microstructure containing many low-angle sub-grain boundaries. These results are generally typical of Al-Mg alloys processed by HPT through small numbers of turns [55].

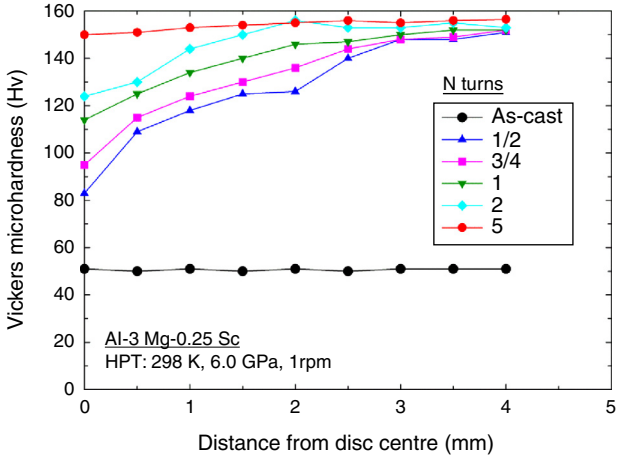

Fig. 4 – Values of the Vickers microhardness for the as-cast alloy and the alloy processed by HPT through up to a maximum of 5 turns plotted against the distance from the centre of each disc.

3.3. *Comparison of the strain introduced during HPT and RCS processing*

During HPT processing, the equivalent von Mises strain, ε_{eq}, introduced in the specimen is given by the relationship [56]

$$\varepsilon_{eq} = \frac{2\pi N r}{h\sqrt{3}} \quad (1)$$

where N is the number of revolutions in HPT processing and r and h are the radius and height (or thickness) of the disc, respectively. Thus, Eq. (1) shows that ε_{eq} is a maximum at the edge of the disc and decreases to zero at the centre of the disc where $r = 0$.

In RCS processing, the strain imparted to the sample is given by [57]

$$\varepsilon = N_p \frac{4}{3} \ln\left(\frac{R+t}{R+0.5t}\right) \quad (2)$$

where N_p is the number of passes in RCS, R is the radius of the semi-circular depressions within the die used to impose the corrugations and t is the thickness of the specimen.

Applying these relationships to the present investigation, the strain in the RCS sample after 8 cycles of processing is ~2.21 and this strain is independent of whether or not the sample is rotated around the longitudinal axis between each pass. By contrast, during HPT processing the equivalent von Mises strain introduced at the edge of the disc is ~3.37 after ½ turn of HPT and ~4.14 after 1 turn. Thus, the strain imparted in this investigation during HPT for 5 turns is significantly larger than the strain imparted in RCS and this is a significant factor in achieving smaller grains, a higher hardness and a greater level of homogeneity when processing by HPT.

4. Discussion

An Al-3Mg-0.25Sc alloy with an initial grain size of ~150 μm was processed by two different SPD techniques: RCS in which a block of material is continuously corrugated and straightened and HPT in which a thin disc is subjected to a high applied pressure and concurrent torsional straining. It should be noted that processing by RCS without any rotation is analogous to applying cyclic tension-compression to the sample and thus should lead to hardening below any monotonic deformation [58]. Nevertheless, when the sample is rotated after each RCS cycle, the deformation is not strictly in tension-compression and the work hardening of the material is then high.

The present results show that both RCS and HPT give significant grain refinement but the final grain sizes are different. In RCS it is possible to produce a grain size of ~0.6 μm by processing through 8 passes provided the material is rotated in a longitudinal sense by 90° between each pass. In HPT the final grain size is much smaller at ~95 nm. Thus, HPT processing is recognized as the optimum procedure for achieving the maximum grain refinement. The smaller grains attained by HPT are consistent with an earlier investigation comparing MAC and HPT where the final grain sizes in an Al-4Cu alloy were ~0.5 μm after processing by MAC through 35 passes at a temperature of 373 K and this contrasted with a grain size of ~0.25 μm after processing by HPT through 5 turns at room temperature [6].

In the present investigation, both RCS and HPT produce a reasonable level of homogeneity but the microstructures after HPT processing were generally more uniform. Thus, processing by HPT produced an array of ultrafine equiaxed grains, whereas processing by RCS produced grain refinement but with the presence of some elongated grains in the absence of any sample rotation. The favourable characteristics of HPT processing by comparison with RCS is attributed to the presence of near uniform simple shear throughout the HPT processing, which contrasts with the unsteady and irregular deformation imposed when processing by RCS. It should be noted that the microhardness results documented in Figs. 2 and 4 are consistent with the observed microstructures. Thus, the grain size is smaller in HPT and this leads, in the saturation condition, to hardness values that are significantly higher in HPT than in RCS.

Despite the clear advantage in processing by HPT, it is important to note that the samples used in HPT processing are generally very small and typically in the form of discs having thicknesses of <1.0 mm. This places an overall limitation on the utilization of samples from HPT processing, whereas, in RCS processing it is feasible to make use of relatively large samples. Furthermore, the hardness values recorded in Fig. 2 for RCS processing, although lower than the values in Fig. 4 for HPT processing, nevertheless show excellent uniformity over the total length of the sample corresponding to a total length of ~80 mm in this investigation. It is reasonable to anticipate that this uniformity will be achieved even when processing much longer sheets.

There have been recent new developments in HPT in attempts to overcome the size limitation which is an inherent feature of this processing method. For example, HPT has been undertaken with small cylindrical samples [15] and continuous processing has been introduced using either strip [59] or wire [60] samples. Alternatively, the recent introduction of incremental HPT provides the opportunity to make use of samples having much larger aspect ratios [61]. It appears that all of these approaches have the potential for significantly increasing the overall viability of the HPT processing method.

5. Summary and conclusions

(1) Experiments were conducted on an Al-3Mg-0.25Sc alloy to provide a direct comparison between two different SPD processing procedures: repetitive corrugation and straightening (RCS) and high-pressure torsion (HPT). The grain size of the alloy in the initial condition was ~150 μm and the hardness was Hv ≈ 50.

(2) The experimental results show that processing by RCS through 8 passes at room temperature produces significant grain refinement with measured average grain sizes of ~0.7 μm when processing without rotation and ~0.6 μm when rotating the sample by 90° in the same sense between each pass. Measurements of the Vickers microhardness after RCS processing showed that the hardness values remained constant along the total length of the sample with values of Hv ≈ 110 when processing

without rotation and Hv ≈ 128 when processing with rotation. There was evidence for some elongated grains in the materials processed by RCS without rotation.

(3) Processing by HPT through one turn at room temperature using a pressure of 6.0 GPa produced a reasonably homogeneous microstructure with equiaxed ultrafine grains having an average size of ~95 nm. As in conventional HPT, the hardness increased rapidly around the periphery of the disc during HPT but the hardness in the central region increased more slowly. There was good microhardness homogeneity throughout the disc after processing through 5 turns with an average hardness of Hv ≈ 150–156.

(4) The results demonstrate that processing by HPT produces a smaller grain size, higher values for the Vickers microhardness and a more homogeneous microstructure than processing by RCS.

Conflicts of interest

The authors declare no conflicts of interest.

Acknowledgements

This work was supported in part by the European Research Council under ERC Grant Agreement No. 267464-SPDMETALS (YH and TGL).

REFERENCES

[1] Valiev RZ, Estrin Y, Horita Z, Langdon TG, Zehetbauer MJ, Zhu YT. Producing bulkultrafine-grained materials by severe plastic deformation. JOM 2006;58(4):33–9.
[2] Valiev RZ, Langdon TG. Principles of equal-channel angular pressing as a processing tool for grain refinement. Prog Mater Sci 2006;51:881–981.
[3] Zhilyaev AP, Langdon TG. Using high-pressure torsion for metal processing: fundamentals and applications. Prog Mater Sci 2008;53:893–979.
[4] Saito Y, Tsuji N, Utsunomiya H, Sakai T, Hong RG. Ultra-fine grained bulk15 aluminum produced by accumulative roll-bonding (ARB) process. Scr Mater 1998;39:1221–7.
[5] Salishchev GA, Zherebtsov SV, Mironov SY, Myshlayev MM, Pippan R. In: Zehetbauer MJ, Valiev RZ, editors. Nanomaterials by severe plastic deformation. Weinheim, Germany: Wiley-VCH; 2004. p. 691.
[6] Xu XC, Zhang Q, Hu N, Huang Y, Langdon TG. Using an Al-Cu binary alloy to compare processing by multi-axial compression and high-pressure torsion. Mater Sci Eng A 2013;588:280–7.
[7] Valiev RZ, Langdon TG. The art and science of tailoring materials by nanostructuring for advanced properties using SPD techniques. Adv Eng Mater 2010;12:677–91.
[8] Estrin Y, Vinogradov A. Extreme grain refinement by severe plastic deformation: a wealth of challenging science. Acta Mater 2013;61:782–817.
[9] Langdon TG. Twenty-five years of ultrafine-grained materials: achieving exceptional properties through grain refinement. Acta Mater 2013;61:7035–59.
[10] Valiev RZ. Superior strength in ultrafine-grained materials produced by SPD processing. Mater Trans 2014;55:13–8.
[11] Valiev RZ, Estrin Y, Horita Z, Langdon TG, Zehetbauer MJ, Zhu YT. Fundamentals of superior properties in bulk NanoSPD materials. Mater Res Lett 2016;4:1–21.
[12] Zhilyaev AP, Lee S, Nurislamova GV, Valiev RZ, Langdon TG. Microhardness and microstructural evolution in pure nickel during high-pressure torsion. Scr Mater 2001;44:2753–8.
[13] Zhilyaev AP, Nurislamova GV, Kim BK, Baró MD, Szpunar JA, Langdon TG. Experimental parameters influencing grain refinement and microstructural evolution during high-pressure torsion. Acta Mater 2003;51:753–65.
[14] Wongsa-Ngam J, Kawasaki M, Langdon TG. A comparison of microstructures and mechanical properties in a Cu-Zr alloy processed using different SPD techniques. J Mater Sci 2013;48:4653–60.
[15] Sakai G, Nakamura K, Horita Z, Langdon TG. Developing high-pressure torsion foruse with bulk samples. Mater Sci Eng A 2005;406:268–73.
[16] Hohenwarter A, Bachmaier A, Gludovatz B, Scheriau S, Pippan R. Technical parameters affecting grain refinement by high pressure torsion. Int J Mater Res 2009;100:1653–61.
[17] Zhu YT, Jiang HG, Huang JY, Lowe TC. A new route to bulk nanostructured metals. Metall Mater Trans A 2001;32:1559–62.
[18] Huang JY, Zhu YT, Jiang HG, Lowe TC. Microstructures and dislocation configurations in nanostructured Cu processed by repetitive corrugation and straightening. Acta Mater 2001;49:1497–501.
[19] Huang JY, Zhu YT, Alexander DJ, Liao XZ, Lowe TC, Asaro RJ. Development of repetitive corrugation and straightening. Mater Sci Eng A 2004;371:35–9.
[20] Rajinikanth V, Arora G, Narasaiah N, Venkateswarlu K. Effect of repetitive corrugation and straightening on Al and Al-0.25Sc alloy. Mater Lett 2008;62:301–4.
[21] Stobrawa J, Rdzawski Z, Gluchowski W, Malec W. Microstructure and properties of CuNi2Si1 alloy processed by continuous RCS method. J Achiev Mater Manuf Eng 2009;37:466–79.
[22] Stobrawa J, Rdzawski Z, Gluchowski W, Malec W. Ultrafine grained strips of precipitation hardened copper alloys. Arch Metall Mater 2011;56:171–9.
[23] Gluchowski W, Stobrawa J, Rdzawski Z, Malec W. Ultrafine grained copper alloys processed by continuous repetitive corrugation and straightening method. Mater Sci Forum 2011;674:177–88.
[24] Sheikh H, Paimozd E, Hashemi SM. Work hardening of Duratherm 600 cobalt superalloy using repetitive corrugation and straightening process. Russ J Non-Ferr Met 2010;51:59–61.
[25] Stobrawa J, Rdzawski Z, Gluchowski W, Malec W. Ultrafine grained strips of CuCr0.6 alloy prepared by CRCS method. J Achiev Mater Manuf Eng 2009;33:166–72.
[26] Stobrawa JP, Rdzawski ZM, Gluchowski W, Malec WW. Microstructure evolution in CRCS processed strips of CuCr0.6 alloy. J Achiev Mater Manuf Eng 2010;38:195–202.
[27] Gluchowski W, Stobrawa JP, Rdzawski ZM. Microstructure refinement of selected copper alloys strips processed by SPD method. Arch Mater Sci Eng 2011;47:103–9.
[28] Pandey SC, Joseph MA, Pradeep MS, Ragahavendra K, Ranganath VR, Venkateswarlu K, et al. A theoretical and experimental evaluation of repetitive corrugation and straightening: application to Al-Cu and Al-Cu-Sc alloys. Mater Sci Eng A 2012;534:282–7.
[29] Sakai G, Horita Z, Langdon TG. Grain refinement and superplasticity in an aluminum alloy processed by high-pressure torsion. Mater Sci Eng A 2005;393:344–51.
[30] Horita Z, Langdon TG. Microstructures and microhardness of an aluminum alloy and pure copper after processing by high-pressure torsion. Mater Sci Eng A 2005;410–411:422–5.

[31] Horita Z, Langdon TG. Achieving exceptional superplasticity in a bulk aluminum alloy processed by high-pressure torsion. Scr Mater 2008;58:1029–32.
[32] Komura S, Furukawa M, Horita Z, Nemoto M, Langdon TG. Optimizing the procedure of equal-channel angular pressing for maximum superplasticity. Mater Sci Eng A 2001;297:111–8.
[33] Horita Z, Furukawa M, Nemoto M, Barnes AJ, Langdon TG. Superplastic forming at high strain rates after severe plastic deformation. Acta Mater 2000;48:3633–40.
[34] Figueiredo RB, Cetlin PR, Langdon TG. Using finite element modeling to examine the flow processes in quasi-constrained high-pressure torsion. Mater Sci Eng A 2011;528:8198–204.
[35] Figueiredo RB, Pereira PHR, Aguilar MTP, Cetlin PR, Langdon TG. Using finite element modeling to examine the temperature distribution in quasi-constrainedhigh-pressure torsion. Acta Mater 2012;60:3190–8.
[36] Kawasaki M, Langdon TG. The significance of strain reversals during processing by high-pressure torsion. Mater Sci Eng A 2008;498:341–8.
[37] Xu C, Horita Z, Langdon TG. The evolution of homogeneity in processing by high-pressure torsion. Acta Mater 2007;55:203–12.
[38] Xu C, Horita Z, Langdon TG. The evolution of homogeneity in an aluminum alloy processed using high-pressure torsion. Acta Mater 2008;56:5168–76.
[39] Kawasaki M, Horita Z, Langdon TG. Microstructural evolution in high purity aluminum processed by ECAP. Mater Sci Eng A 2009;524:143–50.
[40] Xu C, Horita Z, Langdon TG. Microstructural evolution in an aluminum solid solution alloy processed by ECAP. Mater Sci Eng A 2011;528:6059–65.
[41] Iwahashi Y, Horita Z, Nemoto M, Langdon TG. An investigation of microstructural evolution during equal-channel angular pressing. Acta Mater 1997;45:4733–41.
[42] Iwahashi Y, Horita Z, Nemoto M, Langdon TG. The process of grain refinement in equal-channel angular pressing. Acta Mater 1998;46:3317–31.
[43] Mirsepasi A, Nili-Ahmadabadi M, Habibi-Parsa M, Ghasemi-Nanesa H, Dizaji AF. Microstructure and mechanical behavior of martensitic steel severely deformed by the novel technique of repetitive corrugation and straightening by rolling. Mater Sci Eng A 2012;551:32–9.
[44] Wang J, Horita Z, Furukawa M, Nemoto M, Tsenev NK, Valiev RZ, et al. An investigation of ductility and microstructural evolution in an Al-3-% Mg alloy with submicron grain-size. J Mater Res 1993;8:2810–8.
[45] Wang J, Iwahashi Y, Horita Z, Furukawa M, Nemoto M, Valiev RZ, et al. An investigation of microstructural stability in an Al-Mg alloy with submicrometer grain size. Acta Mater 1996;44:2973–82.
[46] Valiev RZ, Musalimov RS, Tsenev NK. The non-equilibrium state of grain-boundaries and the grain-boundary precipitations in aluminum-alloys. Phys Stat Solidi (a) 1989;115:451–7.
[47] Nazarov AA, Romanov AE, Valiev RZ. On the structure, stress-fields and energy of nonequilibrium grain-boundaries. Acta Metall Mater 1993;41:1033–40.
[48] Estrin Y, Molotnikov A, Davies CHJ, Lapovok R. Strain gradient plasticity modelling of high-pressure torsion. J Mech Phys Solids 2008;56:1186–202.
[49] Sabbaghianrad S, Kawasaki M, Langdon TG. Microstructural evolution and the mechanical properties of an aluminum alloy processed by high-pressure torsion. J Mater Sci 2012;47:7789–95.
[50] Wongsa-Ngam J, Kawasaki M, Langdon TG. Achieving homogeneity in a Cu-Zr alloy processed by high-pressure torsion. J Mater Sci 2012;47:7782–8.
[51] Huang Y, Sabbaghianrad S, Almazrouee AI, Al-Fadhalah KJ, Alhajeri SN, Langdon TG. The significance of self-annealing at room temperature in high purity copper processed by high-pressure torsion. Mater Sci Eng A 2016;656:55–66.
[52] Vorhauer A, Pippan R. On the homogeneity of deformation by high pressure torsion. Scr Mater 2004;51:921–5.
[53] Kawasaki M. Different models of hardness evolution in ultrafine-grained materials processed by high-pressure torsion. J Mater Sci 2014;49:18–34.
[54] Sabbaghianrad S, Langdon TG. An evaluation of the saturation hardness in an ultrafine-grained aluminum 7075 alloy processed using different techniques. J Mater Sci 2015;50:4357–65.
[55] Bazarnik P, Huang Y, Lewandowska M, Langdon TG. Structural impact on the Hall–Petch relationship in an Al-5Mg alloy processed by high-pressure torsion. Mater Sci Eng A 2015;626:9–15.
[56] Valiev RZ, Ivanisenko YV, Rauch EF, Baudelet B. Structure and deformation behaviour of Armco iron subjected to severe plastic deformation. Acta Mater 1996;44:4705–12.
[57] Thangapandian N, Balasivanandha Prabhu S, Padmanabhan KA. Effects of die profile on grain refinement in Al-Mg alloy processed by repetitive corrugation and straightening. Mater Sci Eng A 2016;649:229–38.
[58] Coffin LF, Tavernelli JF. The cyclic straining and fatigue of metals. Trans Met Soc AIME 1959;215:794–807.
[59] Edalati K, Horita Z. Continuous high-pressure torsion. J Mater Sci 2010;45:4578–82.
[60] Edalati K, Lee S, Horita Z. Continuous high-pressure torsion using wires. J Mater Sci 2012;47:473–8.
[61] Hohenwarter A. Incremental high pressure torsion as a novel severe plastic deformation process: processing features and application to copper. Mater Sci Eng A 2015;626:80–5.